Variations of large spectral sets; two-dimensional correlation analysis of loadings spectra of principal component analysis[a]

Yongliang Liu,[b] Franklin E. Barton, II,[b*] Brenda G. Lyon[b] and Yud-Ren Chen[c]
[b]*USDA, ARS, Richard B. Russell Research Center, Athens, GA 30604-5677, USA*

[c]*USDA, ARS, Beltsville Agricultural Research Center, Beltsville, MD 20725, USA*

This work attempted to interpret the principal component loadings spectra of principal component analysis on large spectral data sets with multi-variables using two-dimensional (2D) correlation analysis. Three examples of visible/near infrared (NIR) spectra of chicken muscles under different conditions were given and discussed. 2D analysis indicated that characteristic bands from loadings spectra are in good agreement with those from a small number of spectra induced by simple external perturbations. Although some advantages of 2D correlation analysis (such as sequential changes in intensity) were not available, it might still be useful for the understanding of large and complex spectral data sets with multi component variations.

Keywords: two-dimensional correlation analysis, visible/NIR spectroscopy, chicken muscles, principal component loadings, principal component analysis (PCA)

Introduction

Generalised two-dimensional (2D) correlation spectroscopy has been established as a viable means to analyse and extract useful information from conventional one-dimensional spectral data.[1] It has been considerably and successfully applied not only to a variety of optical spectroscopic techniques (infrared, near infrared, Raman, visible, fluorescence) but also for a number of different types of external perturbations (thermal, mechanical, chemical, spatial position, etc) and waveforms.[2]

Most 2D applications, so far, are limited to a small number of spectral data affected by simple and univariate static perturbations. Such an entire data set or smaller subset could accentuate the delicate feature and yield additional information of spectral intensity changes occurring around these particular

[a]*Mention of a product or specific equipment does not constitute a guarantee or warranty by the U.S. Department of Agriculture and does not imply its approval to the exclusion of other products that may also be suitable.*

**Author to whom correspondence should be sent: Dr Franklin E. Barton II, USDA, ARS, Richard B. Russell Research Center, Athens, GA 30604-5677, USA. Tel: 706-546-3497; Fax: 706-546-3607; E-mail: wbarton@qaru.ars.usda.gov.*

ranges. On the other hand, one of the specific challenges might be how to implement 2D correlation analysis in much large spectral sets, which are common in chemometric model developments and actually include diverse fluctuations in chemical and physical components, and to acquire useful information from them. Barton *et al.* developed a statistics-based vibrational correlation spectroscopy and partly addressed some concerns in this subject.[3,4] Meanwhile, as an approach to large samples with at least one known attribute, the use of the average spectra which had close physical or chemical values and then to conduct 2D analysis on physical/chemical variable-dependent spectral intensity changes has been reported.[5] Here, we present an alternative method to explore the variations within a large spectral set by analysing the loadings spectra from principal component analysis (PCA). Visible/near infrared (NIR) spectra of chicken breast muscles, under a variety of treatments, were selected as examples, because muscles are one of the complicated agricultural commodities that vary greatly in colour, chemical, physical and sensory attributes from one portion to another.

Visible/NIR spectroscopy has been developed and applied widely in safety and quality control issues of chicken meat products. Applications include the quantitative evaluation of physical characteristics of heat-treated chicken patties, the prediction of chemical components in chicken muscles, the discrimination of "slow-growing" chickens from "industrial" ones, the identification of "fresh" and "frozen" chicken meats and the classification of chicken carcasses into wholesome and unwholesome classes at the slaughter plant.[6–10] Moreover, 2D correlation analysis was applied to investigate the visible/NIR spectral feature of limited chicken breasts under various conditions, such as cooking, thawing and cold storage as well as diseases.[11–14] Results have shown that 2D visible/NIR analysis cannot only establish the spectral band assignments but can also monitor the complex sequence of events arising from the changes in meats. Furthermore, the visible bands identified through 2D studies have been found to be useful as an indicator of meat colour variation during cooking, irradiation and cold storage.[15–16] The results have developed the relationship between spectral absorption and meat colour structure and also demonstrated the significance of the 2D approach in analysing overlapped and broad absorption bands of meat products.

The objectives of this work were to investigate 2D correlation analysis on loadings spectra of PCA models from visible/NIR spectra of a number of chicken muscles with three different treatments and to compare the results with the earlier reports on visible/NIR spectral intensity variations of chicken breasts induced by single variables.[5,11–14]

Materials and methods

Muscle samples

Example 1. Chicken breasts at various de-bone times[17]

A total of 144 commercially grown, mixed-sex broilers were used in this study. In each of four replications, 36 carcasses were randomly subdivided into four groups of nine carcasses according to the time that the breast muscles were to be removed. Four groups were designated for the post-chill de-boning times of 2, 4, 6 and 24 h. Breast muscles for the 2 h group were removed from carcasses within 10 min of arrival at the laboratory. Carcasses aged at 4, 6 or 24 h prior to muscle removal were kept on ice in containers placed in a 0–2°C cold room until the appropriate de-boning time. Muscles were removed from the left and right sides of each carcass. Right breasts were individually placed in labelled polyethylene heat-and-seal bags, vacuum-sealed and placed in a –30°C freezer prior to subsequent cooking for Warner–Bratzler shear force, cooking loss and sensory evaluation. Meanwhile, left breasts were evaluated for pH, visible/NIR spectral and instrumental colour.

Example 2. Chicken breasts at various storage regimes[5,9]

Five hundred and twenty-five mixed sex, 42 day-old, commercially processed broiler carcasses were obtained from a local plant. Skinless left and right breast fillets were removed from each carcass, and then packaged immediately in polyethylene bags. The bags were placed in five holding chambers set at temperatures of +4, 0, –3, –12, and –18°C for two days storage (Treatment A) and seven days storage (Treatment B). Treatment C samples were held at the

five temperatures for the same seven days as Treatment B but were then stored an additional seven days at –18°C. Following the thawing at +4°C for frozen samples after appropriate storage treatments, the left breasts were used for visible/NIR spectral collection and the right ones were used for Warner–Bratzler shear force and sensory analysis. After treatments A and B (storage two and seven days), samples from +4°C were scanned immediately and breasts from +0, –3, –12 and –18°C were allowed to equilibrate to +4°C and then scanned. Samples from storage Treatment C were tempered back to +4°C and scanned.

Example 3. Chicken breasts at various irradiation dosages[16]

Skinless and boneless chicken breasts were obtained from a local supermarket. Two breasts were vacuum-packaged in an air-permeable package (E-300, Cryovac, Deerfield, IL, USA). All operations were performed in a meat processing room with a temperature of 6 ± 2°C. After packaging, 48 sample packages containing a total of 96 breasts were transferred to a 0°C refrigerator for overnight storage. The packages were randomly divided into eight groups of six packages, with each group containing 12 chicken breasts. One group was used as the non-irradiated control (0 kGy) while the other seven groups were designated for the irradiation process at the target dosage of 0.2, 0.5, 1.0, 2.0, 3.0, 4.0 and 5.0 kGy. Actual absorbed doses were determined by a Bruker EMS 104 EPR Analyser to be 0, 0.18, 0.46, 0.88, 1.77, 2.69, 3.53 and 4.57 kGy. Immediately after irradiation, the chicken breasts were taken out of the radiation chamber and stored in a cooler filled with ice. It took less than three minutes to transport the irradiated meats from the radiation facility to meat processing room for colour (48 samples) and visible/NIR spectral (additional 48 samples) measurement.

Visible/NIR spectroscopic measurement

Samples were scanned on a NIRSystems 6500 monochromator (NIRSystems, Silver Spring, MD, USA) equipped with a sample transport module and a half coarse sample cell. Reflectance measurements were recorded over the 400–2498 nm wavelength range at 2 nm intervals and 32 scans. The instrument was operated by the software package NIRS3 v.4.10 (Infrasoft International, Inc., Port Matilda, PA, USA).

PCA models and 2D correlation analysis of PC loadings spectra

All visible/NIR spectra in Log (1/*R*) mode were transformed into .spc files (Grams file format), were simply offset to zero at the wavelength of 715 nm where the Log (1/*R*) was minimum and then were smoothed (Savitzky–Golay smoothing function and 11 smoothing points) with the use of Grams/32 software (Version 5.2, Galactic Industries Corp., Salem, NH, USA). Each of three spectral sets was loaded into the Grams/32 PLSPlus/IQ package (Version 5.2, Galactic Industries Corp., Salem, NH, USA) and a PCA model was developed in the 410–1850 nm spectral region and with spectral pre-processing of multiplicative scatter correction (MSC) and mean centring (MC). Full cross-validation was used as the validation method.

By looking at a plot of the total percent variance versus the number of factors in PCA statistics, it was found that the first eight principal component (PC) factors accounted for at least 99.2% of the total variance for each spectral data set, although the optimal number of PC factors was suggested to be 16 or 17. Hence, eight spectra, representing the fist eight PC loadings spectra in each of three experiments, were exported from PCA model and used for 2D interpretation.

It is probable that the combination of reflectance mode + MSC +MC does not yield the best separation of samples for each of the different sample sets, because, practically, spectral pre-treatments with derivatives could provide the optimal discriminant results. However, to make a comparison with the earlier 2D observation, raw spectra in reflectance mode were used for developing PCA models.

The 2D correlation analysis was performed using the KG2D correlation program developed by Ozaki *et al.* of the School of Science, Kwansei-Gakuin University, Japan. {AUTHOR QUESTION: Reference? Include in Acknowledgements?] In the 2D approach, dynamic (or difference) spectra, obtained by subtracting the average spectrum of the individual set from each spectrum, were used to develop the generalised 2D correlation spectra.

?

Selection of the minimum threshold level of a contour map is somewhat arbitrary. Some of the fine features in the correlation spectrum could be lost if the threshold is too high, while minor features arising from noise and baseline distortions might be over accentuated if the selected threshold is too low. The threshold of each contour line map was set to 15% of the maximum point of the map.

The generalised 2D correlation method produces two types of spectra: synchronous and asynchronous correlation spectra. A synchronous 2D correlation spectrum characterises the similarity between the sequential variations of spectral intensities. Positive cross peaks (shown in solid lines) indicate that intensities at both wavelengths are either increasing or decreasing together, while negative peaks (shown in dashed lines) mean that one intensity is increasing while the other is decreasing. An asynchronous 2D correlation spectrum reveals the difference between the perturbation-dependent sequential variations of spectral intensities. From the sign of an asynchronous cross peak, it is possible to assign the specific sequence of events occurring at different perturbation variables. It should be noted that only the spectral data resulting from either monotonic increasing or decreasing perturbations can be used to interpret the sequence of spectral changes in asynchronous spectra meaningfully. Hence, in this paper, the positive or negative signs of asynchronous cross peaks derived from the loadings spectra are not discussed.

Results and discussion

Example 1. Chicken breasts at various de-bone times

Acceptably tender breast meat requires a *post-mortem* aging time of 4 to 6 h before de-boning.[18–19] During the *post-mortem* aging of entire carcasses, muscles undergo a number of changes that can affect their quality attributes in colour, texture and flavour.[20–22] The de-boning time related changes have been detected in cooked meats by either trained sensory panels or instrumental measurements.[17,23] Subsequently, both sensory evaluation and instrumental method could be used together to draw conclusions and make decisions about meat quality.

Figure 1 shows the average visible/NIR reflectance spectra of raw chicken breast muscles de-boned at 2, 4, 6 and 24 h *post mortem*. There are at least five strong, broad bands with two (430 and 550 nm) in the visible region (400–750 nm) and three (980, 1195 and 1450 nm) in the NIR region (750–1850 nm). Earlier study on a variety of chicken muscles has concluded that the bands at 430 and 550 nm arise mainly from deoxymyoglobin (DeoxyMb) and oxymyoglobin (OxyMb) species, respectively.[13] Intense bands at 980, 1195 and 1450 nm are most likely due to the second overtone of the O–H stretching mode of water, the second overtones of the C–H stretching modes and the first overtones of the O–H/N–H stretching modes of self-associated and water-bonded OH/NH groups in muscles.[24]

With increasing de-bone time, visible/NIR spectral intensity variations in the 410–1850 nm region are not significant, probably due to the muscles undergoing short *post-mortem* periods (no longer than 24 h) and being freshly cut. Actually, relatively large variations in visible/NIR spectra were observed among the individual breast muscles in each of four groups (not shown). The sensory (chewiness and juiciness etc.) and instrumental (Warner–Bratzler shear value) data from the cooked meats indicated significant differences in the muscles due to the de-boning times.[17] However,

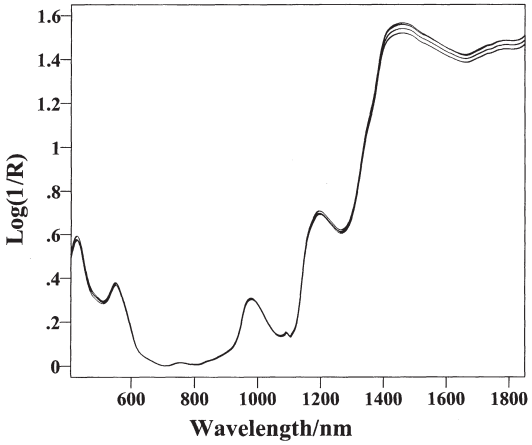

Figure 1. Average visible/NIR reflectance spectra of chicken breasts de-boned at 2, 4, 6 and 24 hr *post mortem* in the 410–1850 nm region.

these changes in magnitude were not linear over the de-boning time-frame.

Figure 2 shows the plots of loading weights for PC factors 1 and 2, which accounted for 87.2% of the variance (PC1 = 58.8% and PC2 = 28.4%). The average spectrum of the entire spectral set is overlaid for comparison. Generally, PC1 has larger positive/negative intensities in the NIR region (1100–1850 nm) than those of the 410–700 nm visible range, while PC2 shows more significant contributions in the visible region. The PC1 spectrum has strong positive loadings at 1200 and 1325 nm, as well as moderate positive loadings at 445, 475, 560, 980 and 1655 nm. Also of importance is the strongly negative loading at 1460 nm, which occurs probably due to opposing contributions from hydrophilic OH/NH groups and hydrophobic CH groups. The PC2 loadings displays pronounced positive correlations with 445, 475 and 560 nm bands and moderate correlations with 1380 and 1655 nm bands.

As muscles generally becomes tender and lose the redness with the de-bone time, it is reasonable to observe such opposite contributions between the bands at 445, 475, 560, 1200 and 1325 nm and the 1460 nm band. Probably, the 1460 nm band arises from components which are responsible for the development of meat tenderness, such as the production of amino acids and alcohols from protein degradation and proteolysis as well as the interaction of water molecules with meat components through hydrogen bonding.[20–22]

Figures 3(a) and 3(b) show synchronous and asynchronous 2D correlation spectra, constructed from PC1 through PC8 in the 410–1850 nm region, respectively. Dominant autopeaks at the diagonal

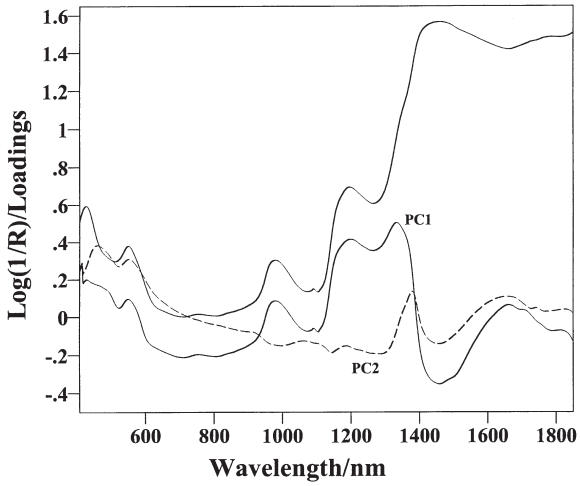

Figure 2. PC1 and PC2 loadings spectra from chicken breasts de-boned at various times (PC1 = 58.8% and PC2 = 28.4%). Average spectrum is overlaid for comparison.

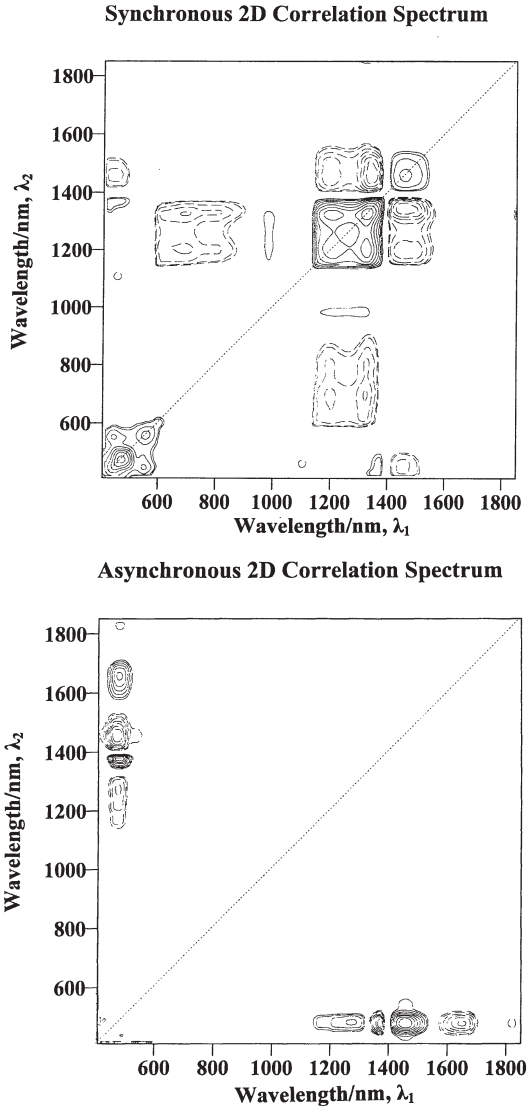

Figure 3. 2D correlation analysis of loadings spectra from chicken breasts de-boned at various times in the 410–1850 nm region: (a) synchronous contour line version; (b) asynchronous contour line version.

position are observed around 475, 560, 1200, 1325 and 1460 nm and cross peaks associated with the autopeaks are also observed at off-diagonal positions [Figure 3(a)]. The appearance of the autopeaks means that the intensities of these bands change very significantly with the PC loadings. Positive cross peaks marked by solid lines are found between the 445 nm band and the 560 nm band, between the 1200 nm band and the 1325 nm band, as well as between the 980 nm band and two bands of 1200 and 1325 nm. Meanwhile, negative cross peaks marked by the dotted lines are observed between the bands coordinated at 1200 and 1325 nm and the absorptions at 690, 790 and 1460 nm. In addition, positive synchronous cross peaks indicate the similar intensity changes between the 445 nm band and the 1345 nm band, whereas negative peaks suggest the opposition in intensity changes between the 445 nm band and the 1460 nm band.

Although no obvious absorptions exist in the 650–900 nm region of Figure 1, Figure 3(a) still reveals correlation peaks at 690 and 790 nm wavelengths. One possible reason is that they may be due to the baseline distortions in loadings spectra, which were caused by the subtle changes in band shape. Physical conditions of muscles and/or chemical

Table 1. Processing of chicken breast muscles and characteristic visible/NIR bands from 2D correlation analysis of PC loadings spectra

	Example 1	Example 2	Example 3	Assignment
Muscle processing	(1) Carcasses storage (< 1 day) (2) Breast removal	(1) Breast removal (2) Breast storage (> 2 days)	(1) Breasts bought in store (2) Irradiation	
Visible / NIR bands (nm)		435	435	DeoxyMb [13]
	445			DeoxyMb [13]
	475	475		MetMb [13]
			485	MetMb [13]
	560	560	560	OxyMb [13]
		635	635	SulfMb [13]
	980	980		OH str. 2nd overtone [24]
			1195	CH str. 2nd overtone [24]
	1200	1200		CH str. 2nd overtone [24]
	1275			2 x CH str.+ CH def. [24]
		1305		2 x CH str.+ CH def. [24]
	1325			2 x CH str.+ CH def. [24]
	1345		1345	2 x CH str.+ CH def. [24]
	1370			2 x CH str.+ CH def. [24]
	1460	1460	1460	OH/NH str. 1st overtone [24]
	1655			CH str. 1st overtone [24]

components are likely causes for such changes in band shape.

Figure 3(b) reveals the existence of asynchronicity among the PC-dependent variations in the 410–1850 nm region. There is an asynchronicity between the 475 nm visible band and at least four NIR bands at 1275, 1370, 1460 and 1655 nm. However, it is impossible to interpret the sequential changes of intensities for these bands meaningfully, because the PC loadings spectra did not result from either monotonic increasing or decreasing perturbations, despite the fact that the spectral set was arranged in increasing order of PC factors. Nevertheless, Figure 3(b) might still provide some interesting points. For example, asynchronous cross peaks are found only between the 475 nm visible band and a number of NIR bands, and none of asynchronous peaks is observed among NIR bands, for example, CH vibration modes (1200 nm or 1325 nm) versus OH/NH vibration (1460 nm). Hence, 2D correlation analysis of loadings spectra identifies the significant bands, which might not be seen easily from individual PC loadings. The characteristic bands are summarised in Table 1. Moreover, general information in Figures 3(a) and 3(b) seems to be identical with previous systematic studies on a small number of visible/NIR spectra of chicken meats and no information is apparently lost. It suggests a potential to characterise the variations in large spectral sets. However, neither band assignments nor sequential changes of spectral intensities can be discussed thoroughly.

Example 2. Chicken breasts at various storage regimes

Processed chicken carcasses are regularly marketed as the fresh refrigerated product (soft flesh), as the chill pack product (hard on surface and soft deep muscle tissues) and as the frozen product (hard frozen throughout). After the consumer has purchased any of these product types, they are usually kept in a refrigerator or placed in a freezer. These different temperature scenarios will cause several changes in meat that can affect its quality.

Visible/NIR reflectance spectra of chicken breast muscles from both storage and frozen-thaw treatments were similar to those in Figure 1 (not shown), except for some minor variations in relative intensities. As expected, the pattern of PC1 and PC2 loadings spectra (depicted in Figure 4) resembles that of Figure 2, but with some variations, because the muscles in this experiment were first cut and then put in different storage environments for more than two days. During the stages of storage and the frozen–thaw process, several significant changes occurred in the muscles, such as discolouration and the development of tenderness. Hence, the relative contribution from the 410–700 nm visible region becomes more apparent in both PC1 and PC2 factors than in Figure 2.

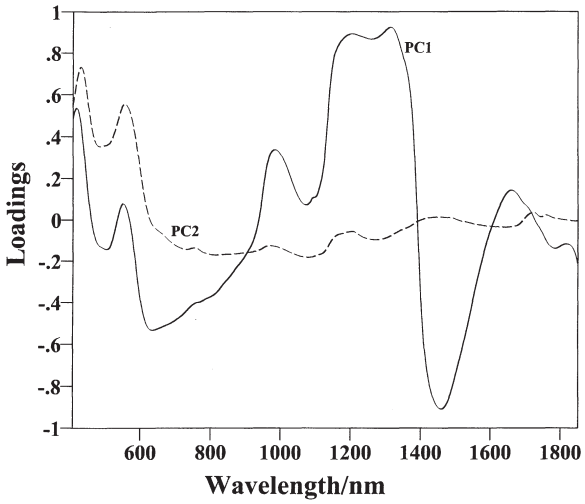

Figure 4. PC1 and PC2 loadings spectra from chicken breasts at various storage regimes (PC1 = 76.2% and PC2 = 13.7%).

Synchronous and asynchronous 2D visible/NIR correlation spectra derived from the spectral set of PC1 through PC8 are given in Figures 5(a) and 5(b), respectively. Autopeaks / cross peaks appearing in Figure 5(a) are reasonably similar to those in Figure 3(a), with an exception of additional autopeaks at 435 and 635 nm. Meanwhile, the NIR bands at 1200, 1305, and 1460 nm are correlated negatively/positively with the visible bands at 435, 475 and 635 nm and with the NIR band at 980 nm.

The presence of a 635 nm band suggests the formation of myoglobin derivatives other than DeoxyMb, OxyMb and MetMb species under the storage regime conditions. The result is consistent

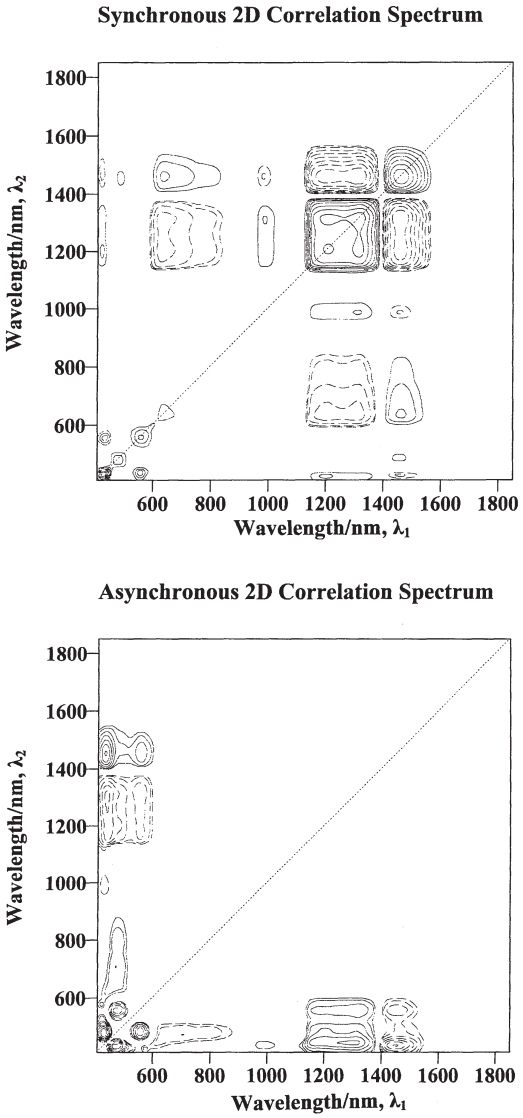

Figure 5. 2D correlation analysis of loadings spectra from chicken breasts at various storage regimes in the 410–1850 nm region: (a) synchronous contour line version; (b) asynchronous contour line version.

with an early study on chicken breasts during cold storage by using visible/NIR spectroscopy and 2D correlation analysis, in which the peak intensity at 635 nm was undetectable in fresh-cut meats and then becomes stronger and distinctive with storage.[13] The 635 nm band has been assigned to SulfMb complexes which are contributed from species such as Sulf-OxyMb, Sulf-DeoxyMb and/or Sulf-MetMb.[13]

The corresponding asynchronous feature [Figure 5(b)] reveals an obvious asynchronicity between the 435 and 560 nm bands and the 475, 1200, 1305 and 1460 nm bands. This is different from Figure 3(b), with asynchronous cross peaks centring at the 435 and 560 nm coordinates. In addition, it confirms that the nature of the absorption at the 475 nm differs from that of the 435 and 560 nm bands.[14]

Example 3. Chicken breasts at various irradiation dosages

Irradiation is an effective method to reduce microbial count but also it can influence the colour appearance of meat significantly.[25,26] Irradiated meat muscles have increased redness and the degree of the increases due to irradiation varies depending on species, muscle type and irradiation dose level.[25] Moreover, the latest study suggested that, with irradiation treatment, MetMb and SulfMb are likely reduced to OxyMb and DeoxyMb species.[16] The relative increase and accumulation of OxyMb species might be responsible for the meat redness. Hence, contributions in the visible region are expected to be dominant in PC1 loadings spectrum

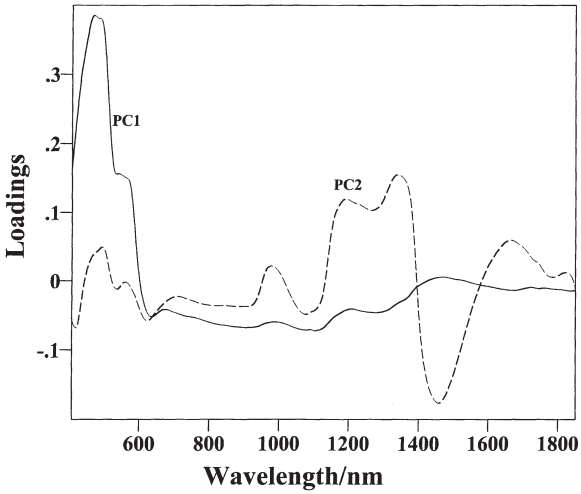

Figure 6. PC1 and PC2 loadings spectra from chicken breasts irradiated at various dosages (PC1 = 52.2% and PC2 = 26.5%).

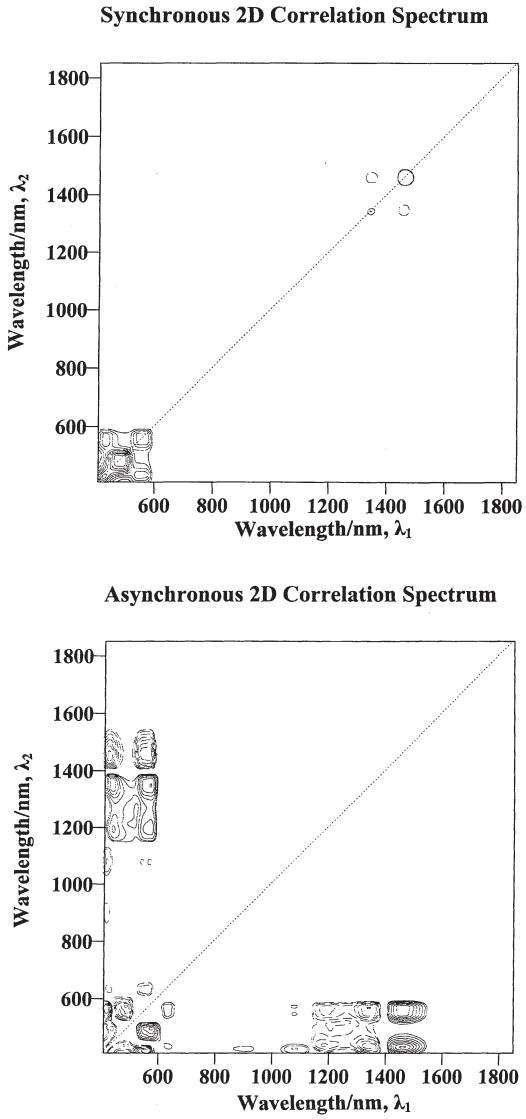

Figure 7. 2D correlation analysis of loadings spectra from chicken breasts irradiated at various dosages in the 410–1850 nm region: (a) synchronous contour line version; (b) asynchronous contour line version.

(Figure 6), contrary to those presented in Example 1 and 2.

Figure 7(a) shows the synchronous 2D correlation spectrum from the data set of PC1 through PC 8 of irradiated meats. It reveals the presence of at least five autopeaks at 435, 485, 560, 1345 and 1460 nm, and all of them appear in Figures 3(a) and 5(a). The corresponding asynchronous spectrum is shown in Figure 7(b). It indicates that two main clusters at the 435 and 560 nm spectral coordinates are accompanied by several asynchronous peaks at the 485, 635, 1195, 1345 and 1460 nm. The existence of these peaks suggests the asynchronicity between DeoxyMb/OxyMb species (435 and 560 nm) and other fractions due to MetMb (485 nm), SulfMb (635 nm), CH groups (1195 nm and 1345 nm) and OH/NH fractions (1460 nm). The observation of the 635 nm band indicates that the samples had been aged/stored. Actually, the samples in this experiment were bought from a local store and the formation of the SulfMb species could be expected. In addition, the absence of the 635 nm autopeak in Figure 7(a) is probably due to a small variation in its amount.

Up to this point, 2D visible/NIR correlation spectra elucidate the common features and differences in PC loadings spectral features of chicken breasts responding with different external treatments. For example, there are at least five common bands at 435, 475, 560, 1200 and 1460 nm in muscles, and their relative intensity variations are apparently associated with the condition of the muscles. One or more visible bands are correlated asynchronously with the NIR bands, and there is no asynchronous peak between NIR bands. Differences among Figures 3, 5 and 7 might indicate the subtle fluctuations of contributions from a number of chemical components in muscles.

Conclusions

The obtained results indicate the possibility of using 2D correlation spectroscopy for interpreting the loadings spectra of PCA models from large visible/NIR spectral data with multi-component variations. It provided consistent observations with a small number of chicken muscles that were induced by simple external perturbations such as cooking, storage and thawing time.

However, important information, such as band assignment and sequential change, is unavailable from such an analysis on loadings spectra because the spectral intensity variations are not induced by increasing or decreasing perturbations. Meanwhile,

some pseudo cross peaks might be introduced due to baseline distortions in loadings spectra and caution must be exercised when one uses PC loadings plots for constructing 2D spectra. Nevertheless, 2D analysis of PCA loadings spectra may be useful for the characterisation of variations in large spectral data.

Acknowledgements

The authors wish to express their sincere thanks to Drs Donald W. Thayer and Xuetong Fan of the Food Safety Unit of ARS/USDA, Pennsylvania and Drs C. E. Lyon and William R. Windham of the Poultry Processing and Meat Quality Research Unit of ARS/USDA, Georgia, for their valuable input into this work.

References

1. I. Noda, *Appl. Spectrosc*. **47,** 1329 (1993).
2. I. Noda, in *Two-dimensional correlation spectroscopy,* Ed by Y. Ozaki and I. Noda. American Institute of Physics, AIP conference proceedings 503, Melville, New York, USA, pp. 3–17 (2000).
3. F.E. Barton, D.S. Himmelsbach, J.H. Duckworth and M.J. Smith, *Appl. Spectrosc*. **46**, 420 (1992).
4. F.E. Barton, D.S. Himmelsbach, A.M. McClung and E.L. Champagne, *Cereal Chem.* **79,** 143 (2001).
5. Y. Liu, F.E. Barton, B.G. Lyon, W.R. Windham and C.E. Lyon, *J. Agri. Food Chem*., in press (2004).
6. H. Chen and B.P. Marks, *J. Food Sci.* **63,** 279 (1998).
7. D. Cozzolino, I. Murray and R. Paterson, *J. Near Infrared Spectrosc.* **4,** 213 (1996).
8. O. Fumiere, G. Sinnaeve and P. Dardenne, *J. Near Infrared Spectrosc.* **8,** 27 (2000).
9. B.G. Lyon, W.R Windham, C.E. Lyon and F.E. Barton, *J. Food Quality* **24,** 435 (2001).
10. Y.R. Chen, R.W. Huffman, B. Park and M. Nguyen, *Appl. Spectrosc*. **50,** 910 (1996).
11. Y. Liu, Y.R. Chen and Y. Ozaki, *J. Agri. Food Chem.* **48,** 901 (2000).
12. Y. Liu and Y.R. Chen, *Meat Sci.* **57,** 299 (2001).
13. Y. Liu and Y. R. Chen, *Appl. Spectrosc*. **54,** 1458 (2000).
14. Y. Liu, Y.R. Chen and Y. Ozaki, *Appl. Spectrosc*. **54,** 587 (2000).
15. Y. Liu and Y.R. Chen, *Meat Sci*. **58,** 395 (2001).
16. Y. Liu, X. Fan, Y.R. Chen and D.W. Thayer, *Meat Sci.* **63,** 301 (2003).
17. Y. Liu, B.G. Lyon, W.R. Windham, C.E. Lyon and E.M. Savage, *Poultry Sci.*, to be submitted.
18. A.A. Klose, R.N. Saye and M.F. Pool, *Poultry Sci.* **50,** 585 (1971).
19. C.E. Lyon, D. Hamm and J.E. Thomson, *Poultry Sci.* **64,** 307 (1985).
20. D.M. Kinsman, A.W. Kotula and B.C. Breidemstein, *Muscle Foods*. Chapman & Hall, New York, USA (1994).
21. R.A. Lawrie, *Meat Science*, 4th Edn. Pergamon Press, Oxford, UK (1985).
22. J. Price and B. Schweigert, *The science of meat and meat products*, 3rd Edn. Food and Nutrition Press, Connecticut, USA (1987).
23. C.E. Lyon and B.G. Lyon, *Poultry Sci.* **69,** 1420 (1990).
24. B.G. Osborne, T. Fearn and P.H. Hindle, *Practical Near Infrared Spectroscopy with Application in Food and Beverage Analysis*, 2nd Edn. Longman Scientific & Technical, Harlow, Essex, UK (1993).
25. K.E. Nanke, J.G. Sebranek and D.G. Olson, *J. Food Sci.* **63,** 1001 (1998).
26. D.W. Thayer, *J. Food Protect.* **56,** 1 (1993).

Received: 6 August 2003
Revised: 12 December 2003
Accepted: 15 December 2003
Web Publication:

Author Question

1. On page 3 you mention the work carried out by Professor Ozaki and his colleagues. Should this be either referenced or mentioned or included in the Acknowledgements.